Nonlinear microscopy with fiber laser continuum excitation

Fredrik Svedberg
Christian Brackmann
Chalmers University of Technology
Department of Chemical and Biological Engineering
Kemivägen 10
412 96 Göteborg, Sweden

Thomas Hellerer
TOPTICA Photonics AG
Lochhamer Schlag 19
82166 Graefelfing (Munich), Germany

Annika Enejder
Chalmers University of Technology
Department of Chemical and Biological Engineering
Kemivägen 10
412 96 Göteborg, Sweden

Abstract. A compact high-power fiber-based femtosecond laser system is presented for coherent anti-Stokes Raman scattering/second-harmonic generation (CARS/SHG) microscopy, and quantitatively compared with a conventional picosecond optical parametric oscillator (OPO)-based system. While the broad spectral width of the femtosecond pulses results in 2.5 times lower image contrast and limited spectral selectivity, lipid stores, myosin, and collagen filaments in living cells can clearly be identified at 60 times lower excitation powers compared to the picosecond system. Visually the images contain the same information. Together with simple operation, small footprint, and low cost, the capabilities of this high-power all-fiber-based laser system promise a more general use of nonlinear microscopy within the biosciences. [DOI: 10.1117/1.3374039]

Keywords: nonlinear microscopy; fiber-based laser; femtosecond laser.

Paper 10031LR received Jan. 20, 2010; revised manuscript received Mar. 1, 2010; accepted for publication Mar. 2, 2010; published online Apr. 6, 2010.

Nonlinear optical properties of biological macromolecules have in recent years been exploited as contrast mechanisms in microscopy.[1] Probed by multiphoton scattering events, e.g., second-harmonic generation (SHG) and coherent anti-Stokes Raman scattering (CARS), they enable label-free chemical imaging of living cells with high 3-D resolution. Assemblies with noncentrosymmetric molecular arrangements, e.g., fibrillar polymers and structural proteins are known to be SHG-active,[2] and collagen content in tumors,[3] cellulose fibers in artificial blood vessels,[4,5] and the detailed arrangement of myosin filaments in muscle tissues,[6] have successfully been monitored by SHG microscopy. In CARS microscopy,[7] contrast is achieved by probing molecular bonds via Raman-active vibrational transitions, such as carbon-hydrogen bonds in the acyl chains of lipids, resulting in a strong signal. Accumulation in preadipocytes,[8] storage in single- and multiple-cell organisms,[9,10] and free fatty acids in cancer-cell membranes,[11] are all examples of lipid studies proving the usefulness of CARS microscopy. Thus, multiple highly relevant applications of nonlinear microscopy have been brought forward in scientific literature. Still, most studies are conducted by a few research groups world-wide that have the competence and advanced equipment required. This is particularly evident for CARS microscopy, involving the coupling of two high-power, short-pulsed laser beams into the microscope with the requirement of precise spatial and temporal overlap in the probe volume.

Early experimental configurations for CARS microscopy were based on temporal synchronization of two separate femtosecond (fs) or picosecond (ps) laser sources.[7] By the launch of a broadly tunable optical parametric oscillator (OPO), pumped by a high-power solid-state laser,[12] inherent synchronization of two picosecond beams was achieved, resulting in a more robust laser source. Still, regular adjustment of the OPO is required. Clearly, to be able to fully focus on the biological problems addressed, there is a great need for laser sources offering simpler operation. One promising route is the use of fiber-based lasers, which require less alignment of the laser itself for operation, deliver high quality laser beams, and can be built more cost effectively. The first attempts toward fiber-based CARS microscopy used a photonic-crystal fiber (PCF) for replacement of the tunable laser source,[13,14] though still requiring a conventional femtosecond laser for pumping the fiber. Another semifiber laser concept was based on a Yb-doped fiber oscillator in series with a cladding-pumped gain fiber emitting enough power to pump a tunable OPO.[15] Both concepts require optical alignment beyond the competence of a nonspecialist. A first all-fiber-based system was presented by Andresen et al. using a gain fiber laser pumping a PCF, allowing for CARS microspectroscopy but with powers too low for imaging.[16] Recently, CARS spectroscopy and microscopy were demonstrated by Marangoni et al.[17] and Pegoraro et al.[18] using spectral compression of the femtosecond output from all-fiber laser systems. This approach increases the spectral selectivity for femtosecond pulse CARS, though including more external optics and lowering the overall power.

In this work we present a compact laser system composed of a femtosecond Er-doped fiber source. Without external pulse compression, we show that the femtosecond output alone allows for chemically specific CARS imaging in a straightforward way with a minimum of free-space optics. The laser system emits high enough power for simultaneous CARS and SHG imaging, i.e., multimodal nonlinear micro-

Address all correspondence to: Annika Enejder, Chalmers University of Technology, Department of Chemical and Biological Engineering, Kemivägen 10, 412 96 Göteborg, Sweden. Tel: 46-31-772-38-52; Fax: 46-31-772-38-01; E-mail: enejder@chalmers.se

1083-3668/2010/15(2)/026026/4/$25.00 © 2010 SPIE

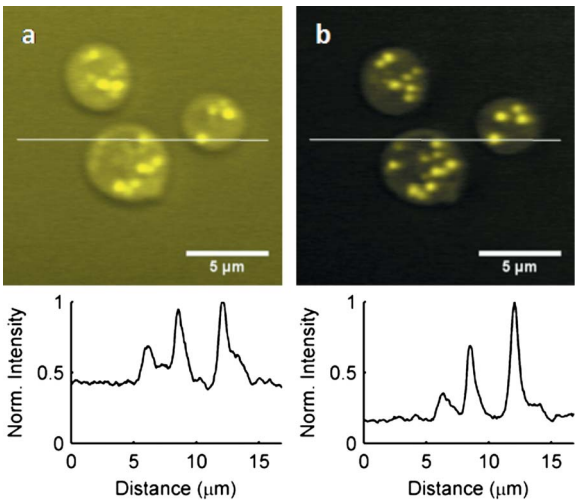

Fig. 1 Direct comparison of CARS images of live yeast cells obtained with (a) the femtosecond and (b) the picosecond laser system. Below each image an intensity line trace along the path indicated in the images is shown.

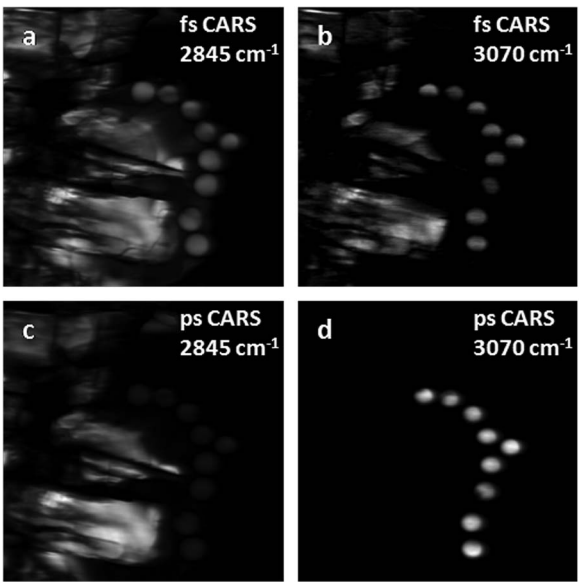

Fig. 2 CARS images of a mixed sample of polystyrene spheres and tripalmitin crystals measured in the CH region. The upper image pair (a) and (b) is measured with the femtosecond laser system at 2845 and 3070 cm^{-1}, respectively. The lower image pair (c) and (d) is measured at the corresponding frequencies using the picosecond laser system. Image size, 100×100 μm.

scopy, here demonstrated for the important biological model systems yeast and *C. elegans*. This extension of a recently launched commercial single-beam laser source has proven useful for two-photon fluorescence microscopy.[19] The frequency-doubled fundamental of the Er-doped pump laser, together with the output of a pumped highly nonlinear fiber (HNLF), allows for different combinations of nonlinear microscopy schemes. The CARS and SHG imaging capabilities of the femtosecond Er-doped fiber laser system are directly and quantitatively compared to the performance of the widely used picosecond Nd:Van laser-pumped OPO system.

The two independent femto- and picosecond laser systems were combined with a single microscope unit. The compact femtosecond light source (FFS series, Toptica Photonics AG, Graefelfing, Germany) is based on a mode-locked Er-doped fiber oscillator that generates 100-fs pulses at 1.56 μm with a repetition rate of 82 MHz. Two fiber amplifier stages seeded by the same oscillator generate two perfectly synchronized output beams for the CARS experiment: the frequency-doubled output with 80-mW average power at 782 nm serves as a pump/probe beam, and the tunable IR continuum (990 to 1100 nm) generated in the HNLF, with 20-mW output power, serves as a Stokes beam. The picosecond laser system, consisting of a solid state pump laser and an OPO, is described in more detail in Enejder, Brackmann, and Svedberg.[20] Briefly, the system consists of a Nd:Van laser (picoTRAIN, High-Q Laser GmbH, Bregens, Austria) that delivers 7-ps pulses at 1064 nm with a repetition rate of 76 MHz. A fraction of the 1064-nm laser beam constitutes the Stokes beam, while the rest is used to synchronously pump a ring-cavity OPO (Levante, APE GmbH, Berlin, Germany) that provides the pump/probe beam tunable in the range of 785 to 845 nm. The femto- and picosecond laser beams, initially following separate beam paths, were aligned into the same inverted microscope (Nikon TE-2000) via the beam scanning unit (Nikon C1) and focused on the sample by the objective (Nikon Plan Fluor 40×, NA 1.30). A flip-mounted mirror positioned in front of the scanner allowed for sequential femto- and picosecond imaging. The signal was collected by an aspherical lens (NA 0.68) in the forward direction and detected by a photomultiplier tube (PMT) (Hamamatsu R6357) equipped with bandpass filters, allowing on-and-off resonance measurements in the CH region using both systems. The powers of the two laser systems were adjusted to give approximately the same CARS signal level on the PMT for a given detector voltage, and powers measured before the microscope were around 5 mW and 300 mW for the femto- and picosecond beams, respectively. The powers at the sample position are typically 10% of these values due to attenuation in the microscope. For excitation of the CH_2 stretching frequency at 2845 cm^{-1} with both laser systems, the femtosecond continuum was centered at 1007 nm and the picosecond OPO was tuned to 817 nm. The laser line widths of the femtosecond beams are 40 nm for the continuum and 5 nm for the frequency doubled; the line widths of both picosecond beams are 0.3 nm. Intrinsically larger line widths are expected for a laser system of shorter pulse duration; however, the fiber laser continuum also obtains additional spectral broadening from dispersion in the HNLF.

The CARS microscopy capabilities of the fiber laser system are shown in Fig. 1 together with a direct comparison with the picosecond system. Figures 1(a) and 1(b) show images of living yeast cells at the CH_2 stretching frequency obtained with the femto- and picosecond systems, respectively, using the specified laser wavelengths. Qualitatively, the images look similar, with the intracellular lipid droplets clearly visible for both cases. Although a higher lipid droplet signal is obtained in the femtosecond image compared to the picosecond image, the latter shows a better signal versus background from the surrounding cell medium. The images

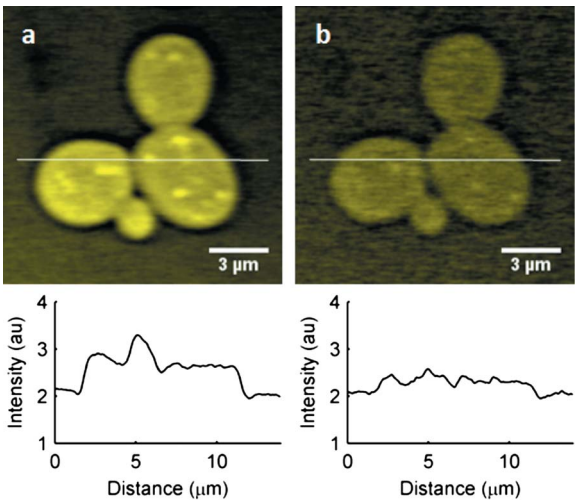

Fig. 3 CARS images of live yeast cells obtained with the femtosecond fiber laser system. Measured at (a) 2845 cm^{-1} and (b) 3070 cm^{-1}. Below each image an intensity line trace along the path indicated in the images is shown.

differ in contrast by a factor of ~2.5, as indicated by the profile below each image. The difference in contrast can be explained by the broader spectral profile of the femtosecond laser, resulting in a higher amount of laser power used for excitation outside the Raman vibrational band, and contributing to a higher unspecific nonresonant background.

To directly compare the spectral selectivity of the femto- and picosecond lasers, CARS images of a sample composed of tripalmitin crystals and polystyrene spheres were collected. Tripalmitin is a saturated triacylglyceride showing a CH_2 symmetric stretch mode at 2845 cm^{-1}, while polystyrene has a symmetric stretch vibration of the C–H bonds in the phenyl ring at 3070 cm^{-1}. Figure 2 shows CARS images collected at the two frequencies using both laser systems. While Figs. 2(a) and 2(b) clearly show that the spectrally broad excitation profile of the femtosecond system generates signal from both sample components when tuned to any of the resonances, the picosecond images, Figs. 2(c) and 2(d), show a clear on-and-off resonance behavior for both sample components. The influence of laser line width on the spectral selectivity of CARS microscopy is well known, and broadband excitation with femtosecond pulses results in less specific imaging.[7] Based on the measured laser emission spectra, the femtosecond system probes a ~400-cm^{-1}-wide band of nonresonant CARS signals together with a small resonant contribution, whereas the picosecond system effectively excites the resonant CARS signal with a ~5-cm^{-1} narrow profile inside the range of the probed vibrational Raman band with a line width of 50 cm^{-1} in the CH region. CARS images of yeast cells obtained with the femtosecond system at 2845 and 3070 cm^{-1} are shown in Figs. 3(a) and 3(b), respectively. Again the high background in the images is due to the broad spectral signature of the femtosecond system, and the CARS signal in lipid droplets is ~1.25 times higher on CH_2 resonance compared to off. Thus, the selectivity obtained with the femtosecond system is sufficient for imaging of lipids probing their vibrations of high cross sections.

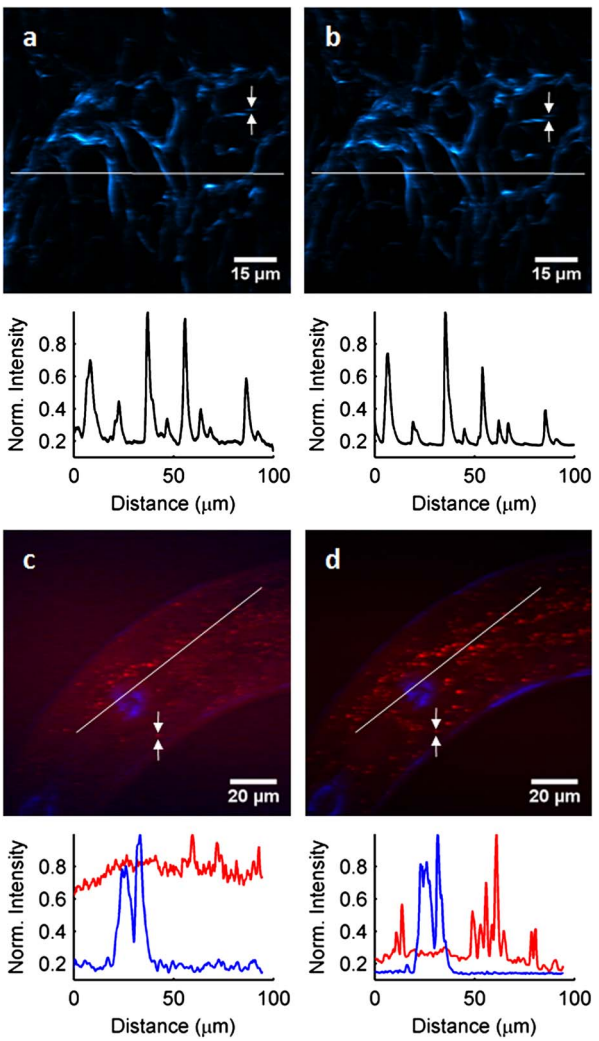

Fig. 4 SHG images of blood vessels from sheep excited by (a) femtosecond pulses and (b) picosecond pulses. Superimposed images of CARS and SHG of *C. elegans* obtained with (c) the femtosecond and (d) the picosecond system. The red color represents CARS and the blue color represents SHG. (Color online only.)

The versatility of the fiber-based laser system also allowed for SHG imaging using the frequency-doubled fiber output at 782 nm. Figure 4(a) shows a SHG image of blood vessels from sheep and Fig. 4(b) the corresponding image acquired with the picosecond OPO at 817 nm. The collagen fibers in the tissue give strong SHG signals, easily generated by both laser systems, and the line traces below the images show that they provide the same amount of detail, although the average excitation power is 60 times lower for the femtosecond system. In contrast to many other fiber lasers, the high output power from the Er-doped fiber even permits multimodal nonlinear microscopy, as shown by the combined CARS and SHG images of *C. elegans* [Figs. 4(c) and 4(d)]. This is an important quality, allowing colocalization of structures with different chemical composition and biological functions. The images provide similar qualitative information, but in this more complex organism, it is clear that the limited specificity for CARS imaging of lipids using the femtosecond system [Fig. 4(c)] makes lipid droplet quantification difficult com-

pared to the corresponding picosecond image [Fig. 4(d)]. This is further demonstrated by the intensity profiles shown below the images. Whereas the lipid droplets in the femtosecond CARS image tend to disappear in the background, the SHG signals generated by the myosin of the nematode muscle tissue still result in high image quality. A laser system combining the improved specificity with picosecond pulses and the facilitated operation of a fiber laser has recently been presented, though with low output powers that could be a limiting factor for its use in SHG and multimodal microscopy.[21]

Although variations in image contrast due to spectral selectivity, no difference in spatial resolution could be detected between the two systems, which mainly is governed by the excitation wavelength and microscope optics, and often in practice, by the pixel dimension. As indicated by the arrows in Fig. 4, the SHG images exhibit fine details of collagen fibers with dimensions of ~400 nm, i.e., close to the diffraction limit, and the CARS images clearly show submicron-sized lipid droplets. The SHG and CARS signals probed inside *C. elegance* nematodes gave similar optical information throughout the sample, indicating no practical difference in penetration depths of the lasers systems.

In conclusion, the femtosecond fiber laser provides a compact and user friendly excitation source for multimodal nonlinear microscopy. Compared to a picosecond system used as a standard for CARS microscopy, the femtosecond system generates images with similar visual information at significantly lower average excitation power. This is beneficial for biological imaging, since photodamage related to linear absorption is minimized while the risk of nonlinear photoinduced changes that benefit from high peak intensities is on the same level as for picosecond excitation.[22] The laser powers here corresponds to peak intensities well below those reported to induced photodamage in cultured cells.[23] For CARS microscopy, we demonstrate that limited specificity is achieved, though sufficient for lipid structures in a simple chemical environment, i.e., biological model systems such as lipid bilayer vesicles and yeast cells. A variety of methods can be implemented to increase the signal sensitivity in CARS microscopy by suppressing the nonresonant background.[24] In the case of femtosecond excitation, relatively complex time-resolved detection can utilize the different temporal behavior of the resonant and nonresonant contributions to completely remove the nonresonant part, although also significantly attenuating the resonant part.[25] Nevertheless, with technical improvements of the laser in continuum tunability, allowing CARS background measurements in the silent region, and filtering of the continuum emission using suitable bandpass filters to reduce nonresonant excitation, the femtosecond Er-fiber laser has the potential to become a future basic excitation source for nonlinear microscopy.

References

1. W. R. Zipfel, R. M. Williams, and W. W. Webb, "Nonlinear magic: multiphoton microscopy in the biosciences," *Nat. Biotechnol.* **21**, 1369–1377 (2003).
2. W. Mohler, A. C. Millard, and P. J. Campagnola, "Second harmonic generation imaging of endogenous structural proteins," *Methods* **29**, 97–109 (2003).
3. E. Brown, T. McKee, E. diTomaso, A. Pluen, B. Seed, Y. Boucher, and R. K. Jain, "Dynamic imaging of collagen and its modulation in tumors *in vivo* using second-harmonic generation," *Nat. Med.* **9**, 796–800 (2003).
4. R. M. Brown, A. C. Millard, and P. J. Campagnola, "Macromolecular structure of cellulose studied by second-harmonic generation imaging microscopy," *Opt. Lett.* **28**, 2207–2209 (2003).
5. C. Brackmann, A. Bodin, M. Åkeson, P. Gatenholm, and A. Enejder, "Visualization of the cellulose biosynthesis and cell integration into cellulose scaffolds," *Biomacromolecules* **11**, 542–548 (2010).
6. S. V. Plotnikov, A. C. Millard, P. J. Campagnola, and W. A. Mohler, "Characterization of the myosin-based source for second-harmonic generation from muscle sarcomeres," *Biophys. J.* **90**, 693–703 (2006).
7. J. X. Cheng and X. S. Xie, "Coherent anti-Stokes Raman scattering microscopy: Instrumentation, theory, and applications," *J. Phys. Chem. B* **108**, 827–840 (2004).
8. X. L. Nan, J. X. Cheng, and X. S. Xie, "Vibrational imaging of lipid droplets in live fibroblast cells with coherent anti-Stokes Raman scattering microscopy," *J. Lipid Res.* **44**, 2202–2208 (2003).
9. T. Hellerer, C. Axang, C. Brackmann, P. Hillertz, M. Pilon, and A. Enejder, "Monitoring of lipid storage in Caenorhabditis elegans using coherent anti-Stokes Raman scattering (CARS) microscopy," *Proc. Natl. Acad. Sci. U.S.A.* **104**, 14658–14663 (2007).
10. C. Brackmann, J. Norbeck, M. Åkeson, D. Bosch, C. Larsson, L. Gustafsson, and A. Enejder, "CARS microscopy of lipid stores in yeast: the impact of nutritional state and genetic background," *J. Raman Spectrosc.* **40**, 748–756 (2009).
11. T. T. Le, T. B. Huff, and J. X. Cheng, "Coherent anti-Stokes Raman scattering imaging of lipids in cancer metastasis," *BMC Cancer* **9**, 42 (2009).
12. F. Ganikhanov, S. Carrasco, X. S. Xie, M. Katz, W. Seitz, and D. Kopf, "Broadly tunable dual-wavelength light source for coherent anti-Stokes Raman scattering microscopy," *Opt. Lett.* **31**, 1292–1294 (2006).
13. H. N. Paulsen, K. M. Hilligsoe, J. Thogersen, S. R. Keiding, and J. J. Larsen, "Coherent anti-Stokes Raman scattering microscopy with a photonic crystal fiber based light source," *Opt. Lett.* **28**, 1123–1125 (2003).
14. T. W. Kee and M. T. Cicerone, "Simple approach to one-laser, broadband coherent anti-Stokes Raman scattering microscopy," *Opt. Lett.* **29**, 2701–2703 (2004).
15. K. Kieu, B. G. Saar, G. R. Holtom, X. S. Xie, and F. W. Wise, "High-power picosecond fiber source for coherent Raman microscopy," *Opt. Lett.* **34**, 2051–2053 (2009).
16. E. R. Andresen, C. K. Nielsen, J. Thogersen, and S. R. Keiding, "Fiber laser-based light source for coherent anti-Stokes Raman scattering microspectroscopy," *Opt. Express* **15**, 4848–4856 (2007).
17. M. Marangoni, A. Gambetta, C. Manzoni, V. Kumar, R. Ramponi, and G. Cerullo, "Fiber-format CARS spectroscopy by spectral compression of femtosecond pulses from a single laser oscillator," *Opt. Lett.* **34**, 3262–3264 (2009).
18. A. F. Pegoraro, A. Ridsdale, D. J. Moffatt, J. P. Pezacki, B. K. Thoma, L. Fu, L. Dong, M. E. Fermann, and A. Stolow, "All-fiber CARS microscopy of live cells," *Opt. Express* **17**, 20700–20706 (2009).
19. D. Träutlein, F. Adler, K. Moutzouris, A. Jeromin, A. Leitenstorfer, and E. Ferrando-May, "Highly versatile confocal microscopy system based on a tunable gfemtosecond Er:fiber source," *J. Biophoton.* **1**, 53–61 (2008).
20. A. Enejder, C. Brackmann, and F. Svedberg, "Coherent anti-Stokes Raman scattering microscopy of cellular lipid storage," *IEEE J. Sel. Top. Quantum Electron.* (in press).
21. G. Krauss, T. Hanke, A. Sell, D. Träutlein, A. Leitenstorfer, R. Selm, M. Winterhalder, and A. Zumbusch, "Compact coherent anti-Stokes Raman scattering microscope based on a picosecond two-color Er:fiber laser system," *Opt. Lett.* **34**, 2847–2849 (2009).
22. H. J. Koester, D. Baur, R. Uhl, and S. W. Hell, "Ca^{2+} fluorescence imaging with pico- and femtosecond two-photon excitation: signal and photodamage," *Biophys. J.* **77**, 2226–2236 (1999).
23. Y. Fu, H. Wang, R. Shi, and J. X. Cheng, "Characterization of photodamge in coherent anti-Stokes Ramans scattering microscopy," *Opt. Express* **14**, 3942–3951 (2006).
24. M. Müller and A. Zumbusch, "Coherent anti-Stokes Raman scattering microscopy," *ChemPhysChem* **8**, 2156–2170 (2007).
25. A. Volkmer, L. D. Book, and X. S. Xie, "Time-resolved coherent anti-Stokes Raman scattering microscopy: Imaging based on Raman free induction decay," *Appl. Phys. Lett.* **80**, 1505–1507 (2002).